Analysis of Unsteady Inviscid Diffuser Flow with a Shock Wave

V. Yang* and F. E. C. Culick†
California Institute of Technology, Pasadena, California

A finite difference scheme with a shock-fitting algorithm has been used to investigate unsteady inviscid flow with a shock in an inlet diffuser. The flowfield consists of three different regions: the supersonic and the subsonic regions, and a region containing both air and liquid fuel droplets, separated by a normal shock wave and a fuel injection system. The analysis is based on a two-phase, quasi-one-dimensional model. The response of a shock wave to various disturbances has been studied, including large-amplitude periodic oscillations and pulse perturbations.

Nomenclature

a = speed of sound
A = cross-sectional area
c_l = specific heat of fuel
c_p = constant pressure specific heat of air
d = diameter of fuel droplet
f = frequency
F_p = drag force between air and fuel droplets
L_d = length of diffuser
L_f = position coordinate of fuel injector
M = Mach number
p = pressure
P_s = defined by Eq. (29), Ref. 11
P_+, P_- = amplitudes of rightward and leftward traveling pressure waves, respectively
Q_p = heat-transfer rate between air and fuel droplets
R_m = mass response function, defined by Eq. (11)
s = entropy
t = time
T = temperature
T_r = acoustic transmission coefficient, defined by Eq. (16)
u = velocity
U_s = defined by Eq. (30), Ref. 11
v_s = velocity fluctuation of normal shock
x = position coordinate along the axis of the diffuser
x_s = position fluctuation of normal shock
β = acoustic reflection coefficient of normal shock presented to downstream disturbance
γ = ratio of specific heats
δp = pressure fluctuation
ΔS = dimensionless entropy, defined by Eq. (9)
η = ratio of airflow through the injector to the main flow
ρ = density
ω = angular frequency
ω_g = rate of air injected into the main flow
ω_p = rate of liquid fuel injected into the main flow
Ω = dimensionless angular frequency, defined by Eq. (8)

Superscripts

$(\_)^*$ = sonic condition
$(\bar{\ })$ = average value
$(\ )'$ = fluctuation

Subscripts

e = incident disturbance
ex = value at exit of diffuser
in = value at entrance of diffuser
p = liquid phase
s = value at normal shock
sg = value at port of fuel injector
t = transmitted disturbance
1,2 = value upstream and downstream of normal shock, respectively

Introduction

UNSTEADY inlet diffuser flow with a shock wave has received considerable attention in recent investigations of longitudinal combustion instabilities in ramjet engines.[1] As a consequence of pressure fluctuations generated by combustion processes, the stability margin of the inlet diffuser may have to be increased to accommodate perturbations of the shock system. In the work reported herein, a finite difference scheme with a shock-fitting algorithm is used to study unsteady behavior of the inlet flow. The formulation is directed specifically to obtaining results required in the analysis of unsteady motions in engines.

In a continuing experimental program, Sajben and coworkers[2-4] have reported extensive, detailed observations in the transonic range. They have summarized the features of the flowfields under various conditions. Both self-sustaining and mechanically induced oscillations were investigated. Schadow et al.[5] examined oscillations in a research dump combustor with special attention focused on the inlet shock/acoustic wave interaction. Two kinds of data have been taken: the acoustic wave structure and the characteristics of the inlet shock.

Several analyses of the problem have been carried out. Adamson et al.[6] obtained systematic solutions for large-amplitude shock-wave motion in a two-dimensional transonic flow using methods of matched asymptotic expansions. The same approach was later extended to include boundary-layer displacement effects,[7] and shock-wave/boundary-layer interaction.[8] In Refs. 9 and 10, numerical solutions of Navier-Stokes equations for multidimensional transonic/supersonic flows were reported. The detailed information obtained provides a better understanding of the flowfields, especially under conditions when flow separation occurs.

Received March 16, 1984; revision received Aug. 17, 1984.

*Postdoctoral Research Fellow.
†Professor of Applied Physics and Jet Propulsion. Associate Fellow AIAA.

For linear stability analysis of unsteady motions in an engine, the boundary condition at the upstream end of the diffuser is conveniently expressed as the admittance function of a normal shock wave. A pressure fluctuation incident on the shock causes a velocity fluctuation. The admittance function is proportional to the ratio of the velocity to the pressure fluctuations. Culick and Rogers[11] analyzed the problem of small-amplitude motions of a normal shock in one-dimensional flow. Results for the admittance function were given for two cases: inviscid flow, and a case which might be regarded as a crude approximation to the influences of separation. The work reported herein begins with essentially the same model of the flow, but numerical results are obtained for finite-amplitude motions.

Figure 1 shows the idealized inlet system considered, consisting of a convergent-divergent channel and a fuel injection system. Air is delivered to a diffuser, becomes sonic at the throat, then accelerates supersonically in the divergent section. After passing through a normal shock wave, the flow becomes subsonic and decelerates to the exit, which may represent the inlet/combustor interface. Either fuel or fuel-air mixture, depending on the injector and atomizer used, is injected into the main flow downstream of the shock to provide the necessary combustible mixture. As a first approximation, the gas flow is treated as inviscid. Neglect of the viscous boundary layers is an obvious deficiency, which will be corrected in subsequent work.

Within this representation, interaction between the inlet and combustor may be visualized as follows. Unsteady combustion generates a pressure wave propagating upstream and causes the shock to oscillate about its mean position. As a consequence, the induced shock motion produces fluctuations of entropy and mass flow rate, which, together with the reflected pressure wave, may augment or attenuate the initial disturbance. The purpose of this paper is to examine this process with the following objectives: 1) to study the response of a normal shock wave to various disturbances; 2) to analyze the changes of flow properties, such as entropy and mass flow rate, due to shock motion; and 3) to examine the influences of liquid fuel droplets and wall air jet injected downstream of the shock wave. The coupling between the inlet and processes in the combustion chamber are not treated here.

Formulation

To facilitate numerical calculation, only the flow downstream of the throat is considered. The flowfield therefore consists of three different regions shown in Fig. 1: the supersonic and subsonic regions, separated by a normal shock; and a region containing both air and fuel droplets. The fuel droplets are assumed to have uniform size and to be distributed over the entire cross-sectional area, the initial phase of fuel jet breakup and multidimensional effects being ignored. For some systems, preparation of fuel droplets may be achieved outside the diffuser. In that case, a mixture of air and fuel, rather than pure fuel, is injected into the mainstream. Both cases are accommodated.

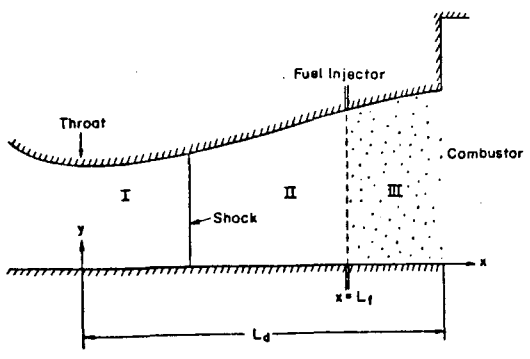

Fig. 1 Schematic diagram of inlet diffuser.

The analysis is based on a two-phase, quasi-one-dimensional model. If we neglect viscous boundary-layer effects and droplet vaporization, the equations governing the gas and the liquid flows can be expressed in the following conservation and nonconservation forms.

Gas phase:

$$\frac{\partial \rho}{\partial t}+\frac{1}{A}\frac{\partial(\rho u A)}{\partial x}=\omega_g \tag{1}$$

$$\frac{\partial(\rho u)}{\partial t}+\frac{1}{A}\frac{\partial}{\partial x}\left[\left(\frac{p}{\gamma}+\rho u^2\right)A\right]=\frac{p}{\gamma A}\frac{\mathrm{d}A}{\mathrm{d}x}+F_p+u_{sg}\omega_g \tag{2}$$

$$\frac{\partial}{\partial t}\left[\rho\left(\frac{T}{\gamma(\gamma-1)}+\frac{u^2}{2}\right)\right]+\frac{1}{A}\frac{\partial}{\partial x}\left[\rho u A\left(\frac{T}{\gamma(\gamma-1)}+\frac{u^2}{2}\right)\right]$$
$$=\frac{-1}{\gamma A}\frac{\partial(upA)}{\partial x}+\omega_g\left(\frac{T_{sg}}{\gamma-1}+\frac{u_{sg}^2}{2}\right)+\frac{Q_p}{\gamma-1}+u_pF_p \tag{3}$$

Liquid phase:

$$\frac{\partial \rho_p}{\partial t}+\frac{\partial(\rho_p u_p)}{\partial x}=\omega_p-\frac{\rho_p u_p}{A}\frac{\mathrm{d}A}{\mathrm{d}x} \tag{4}$$

$$\frac{\partial u_p}{\partial t}+u_p\frac{\partial u_p}{\partial x}=-\frac{F_p}{\rho_p} \tag{5}$$

$$\frac{\partial T_p}{\partial t}+u_p\frac{\partial T_p}{\partial x}=-\frac{Q_p}{\rho_p c_l} \tag{6}$$

The flow properties are normalized with respect to their quantities at the entrance except the velocity which is referenced to the speed of sound. Note that the mass source terms ω_g and ω_p are introduced only at the injector position ($x=L_f$), and the momentum and heat-transfer coupling terms F_p and Q_p vanish in regions I and II.

Specification of Boundary Conditions

In order to solve this problem, three boundary conditions must be specified at both boundaries for each phase. These conditions can be formulated by considering: 1) physical situations, 2) compatibility relations obtained from the method of characteristics, and 3) numerical one-sided differences.[12,13] For the gas phase, the conservation equations are totally hyperbolic with the existence of three distinct eigenvalues. Therefore, the upstream boundary conditions are determined by specifying three physical quantities—the Mach number, static pressure, and temperature—since there is no characteristic line running from the interior region to the boundary. At the downstream end, the flow is subsonic. Two characteristic lines run from the interior region to the exit; only the static pressure needs to be specified.

Because the liquid droplets are dispersed, no signal can propagate through them. The governing equations change from totally hyperbolic to hyperbolic; the three characteristic lines collapse into one. This suggests using a one-sided difference for the calculation of the downstream boundary conditions for the liquid phase. Detailed analysis shows that the one-sided difference has the same virtue as the liquid-phase compatibility relation. The conditions at the upstream boundary ($x=L_f$) are determined from the physical requirements set by the convection of droplets downstream.

Numerical Method

The basis for the analysis is a numerical program originally developed for treating one-dimensional nonlinear combustion instability in solid propellant rocket motors.[12] Recently, this program has been improved to accommodate steep-fronted waves by employing a combined finite difference operation.[14]

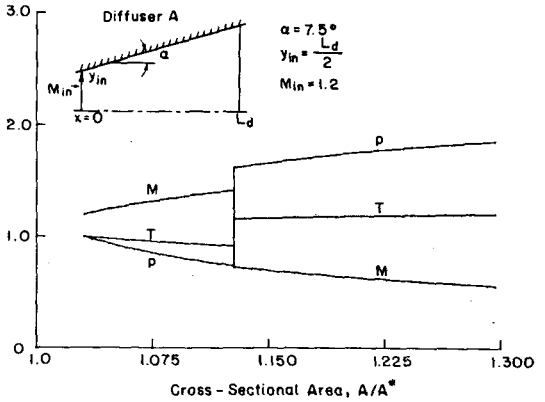

Fig. 2 Distributions of mean flow properties (diffuser A).

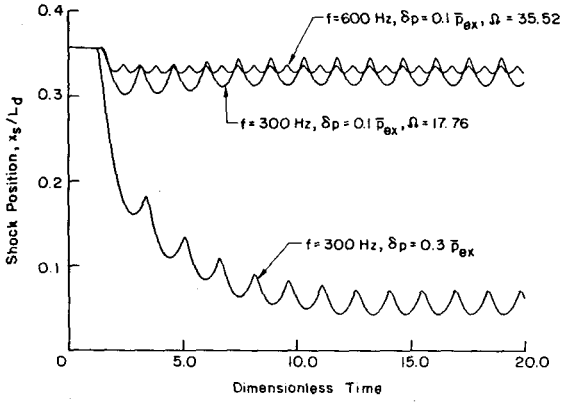

Fig. 3 Instantaneous shock position (diffuser A).

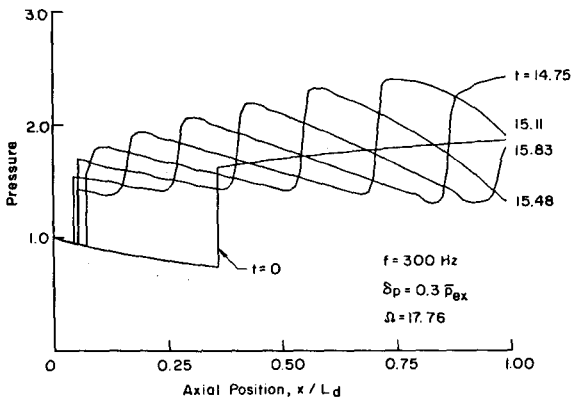

Fig. 4 Pressure distributions at various times within one cycle of oscillation (diffuser A).

The conventional two-step Lax-Wendroff method is hybridized with Harten and Zwas' first-order scheme and further modified by an artificial compression correction.[15] The spurious pre- and postshock oscillations produced by second-order finite difference approximations are greatly reduced. Because of its remarkable shock-capturing feature, the scheme is applied first to solve for steady flowfields.

For unsteady problems, direct application of that method is accompanied by two problems. First, the shock transition requires a small number of computational grids. The flow properties immediately in front of and behind the shock are not well defined. Second, there are two time scales involved in the calculation: τ_{sh} and τ_e. τ_{sh} is the time required for a shock to pass through a grid, and τ_e is associated with an external disturbance. Unless very fine meshes are used, i.e., $\tau_{sh} \ll \tau_e$, the crude time resolution of shock motion may produce false information. To overcome these problems and improve numerical efficiency, a shock-fitting algorithm has been incorporated.

The shock-fitting technique[16] treats the shock as an internal boundary, separating the supersonic and subsonic regions. The Rankine-Hugoniot equations together with four characteristic relations, three in the supersonic region and one in the subsonic region, suffice to provide the required boundary conditions for the finite difference scheme on each side. The motion of the shock front is determined as part of the solution.

The numerical calculation starts with application of the self-adjusting hybrid scheme. As soon as the shock is captured and reaches its steady condition, the shock-fitting algorithm is activated to refine the solution. This has proved to be an effective procedure, producing accurate results with modest costs.

Discussion of Results

Calculations have been carried out for two different diffusers, referred to as A and B, respectively. Diffuser A has a linear area distribution,

$$\frac{A(x)}{A_{in}} = 1 + k\left(\frac{x}{L_d}\right) \tag{7}$$

where L_d is the length of the diffuser from the entrance to the exit. Diffuser B is a convergent-divergent nozzle with a flat bottom and a contoured top wall described in Ref. 4. For each case, the analysis is applied first to compute the flowfield under steady conditions. The response of a shock wave to various disturbances and its associated influences on the flowfield are then examined in detail.

Figure 2 shows the distributions of the mean flow properties in diffuser A with only the gas flow accounted for. The shock-fitting scheme functions well, confining the numerical error within 0.10%. At $t=0$ a sinusoidal pressure oscillation is imposed at the exit, simulating a pressure fluctuation induced by combustion instability. After the time required for the disturbance to travel upstream to the shock, the shock begins to oscillate about its mean position. The local pressure and velocity fluctuations just downstream of the shock are of course different from those existing at the exit and exhibit features due to the nonlinear behavior of the shock and the nonuniformity of the mean flowfield. Figure 3 shows the instantaneous position of the shock for downstream disturbances having different frequencies and amplitudes. The strong influences of frequency and amplitude on the average position are evident; lower frequency and higher amplitude tend to displace the shock toward the throat, unfavorable for the performance of an inlet.

The upstream excursion of the shock shown in Fig. 3 at first seems unreasonably large. Due to the average displacement, the entropy production at the shock during oscillations is less than that for the shock in the initial steady state. Thus, the stagnation pressure loss is less. It would appear, then, that the average exit pressure should be higher in the unsteady flow. This is not in agreement with the requirement imposed in the calculations that the average ambient pressure at the exit is the same in the steady and unsteady flows.‡ That the results are in fact consistent is shown by Figs. 4 and 5.

Figure 4 shows the pressure distributions at four times during one cycle, including the extreme excursions and two intermediate positions of the shock. Due to the nonlinear gasdynamics, the oscillation imposed at the exit develops into a steep-fronted wave as it propagates upstream. The associated entropy production and stagnation pressure loss

‡The authors are indebted to the reviewer for noting this apparent paradox.

compensate the average changes caused by the displacement of the normal shock. This reasoning is verified by calculation of the average pressure, shown in Fig. 5. Curves A and B are the distributions for isentropic steady flows. The time-averaged distribution correctly joins the exit pressure and the value immediately downstream of the average position of the unsteady shock.

The shock response depends strongly on the local diffuser shape. Earlier work[11] has shown that the dimensionless frequency Ω, defined as

$$\Omega = \frac{\omega}{\bar{a}_2} \Big/ \left[\frac{1}{A}\frac{dA}{dx}\right]_{\text{shock}} \tag{8}$$

plays an important role. As a check of the numerical analysis described here, the results for the admittance function given in Ref. 11 for small-amplitude motion have been reproduced. These show that the response of the shock increases if Ω is decreased. According to Eq. (8), this happens if the fractional change of cross-sectional area is increased. For the frequencies chosen here, the values of Ω for the two diffusers treated here are given in Table 1.

Thus, one would anticipate that the shock wave in diffuser B should be more responsive. Comparison of the results shown in Fig. 6 (diffuser B) and Fig. 3 (diffuser A) confirms this conclusion.

Oscillation of Entropy

Entropy fluctuations are generated as a consequence of shock motion due to a pressure disturbance, and are convected downstream by the mean flow. In turn, these may produce pressure waves when passing through a region of nonuniform velocity. From the results for temperature and pressure, the entropy fluctuations can be determined from the following thermodynamic relation:

$$\Delta S \equiv \frac{s_2 - \bar{s}_2}{c_p} = \ell n \frac{T_2}{\bar{T}_2} - \frac{\gamma - 1}{\gamma} \ell n \frac{p_2}{\bar{p}_2} \tag{9}$$

The induced entropy fluctuation is usually very small except for a strong shock. For example, for diffuser A and the unsteady motions shown in Fig. 3, the entropy response function, defined as the ratio $\Delta S/(\Delta p_2/\bar{p}_2)$, has magnitude less than 0.1.

Figure 7 shows the entropy distributions at various times during a cycle of oscillation in diffuser A for the case illustrated in Figs. 4 and 5: $f = 300$ Hz and $\delta p = 0.3\bar{p}_{ex}$. The fluctuations are not smooth because they contain contributions generated at the shock, which propagate downstream with the mean flow, and contributions from the local waves as argued in the preceding section.

Table 1 Values of Ω for two diffusers

	Ω	
Diffuser	300 Hz	600 Hz
A	17.76	35.52
B	2.475	4.950

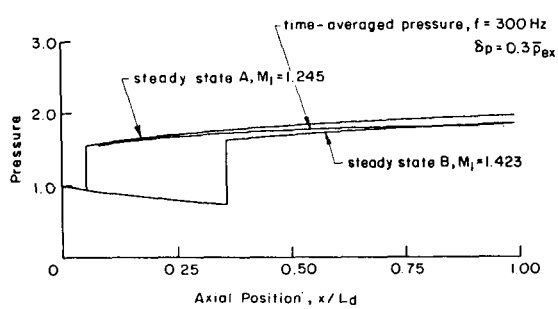

Fig. 5 Time-averaged pressure distributions (diffuser A).

Oscillation of Mass Flow Rate

Even for a fixed mass flow rate upstream of the shock, an oscillation will occur in the downstream region due to the shock motion. To first-order accuracy, the fluctuation of mass flow rate can be written as

$$\Delta \dot{m} = \dot{m}_1 - \dot{m}_2 = (\bar{\rho}_1 - \bar{\rho}_2) v_s' A_s \tag{10}$$

Combination of the above equation with the expression for the incident pressure fluctuation p_e', which is given in Ref. 11,

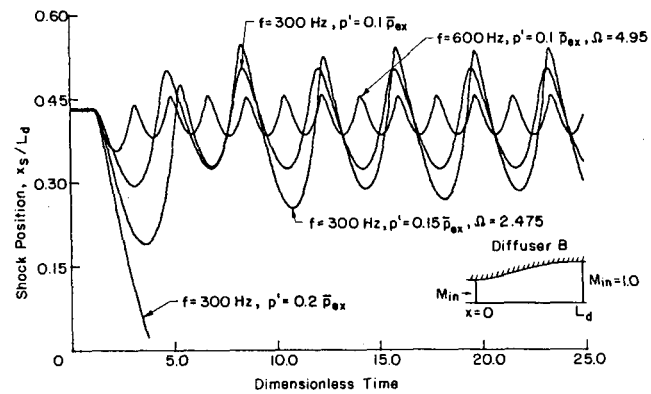

Fig. 6 Instantaneous shock position (diffuser B).

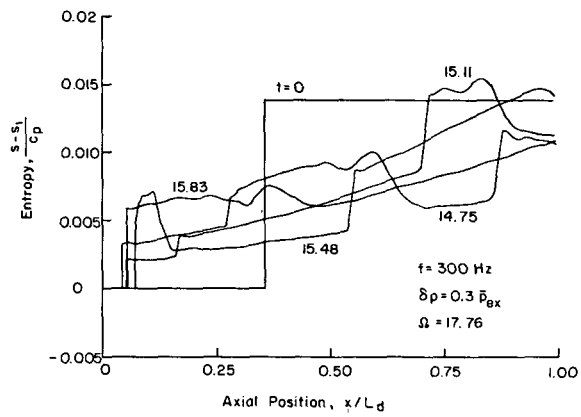

Fig. 7 Entropy distributions at various times within one cycle of oscillation (diffuser A).

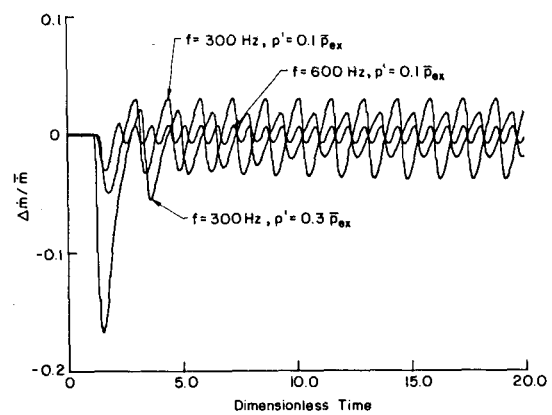

Fig. 8 Oscillation of mass flow rate behind a shock (diffuser A).

and rearrangement of the result, produce a formula for the mass response function.

$$R_m \equiv \frac{\Delta\dot{m}/\bar{\dot{m}}}{p_e'/\bar{p}_2} = \frac{\left(\frac{\bar{p}_2}{\bar{p}_1}-1\right)\left(\frac{\bar{a}_2}{\bar{a}_1}\right)\frac{i\Omega}{\bar{M}_1}}{\frac{4\gamma\bar{M}_1}{\gamma+1}\left(\frac{\bar{p}_1}{\bar{p}_2}\right)\left(\frac{\bar{a}_2}{\bar{a}_1}\right)i\Omega + P_s} \tag{11}$$

where P_s is a function of $\bar{M}_1$, defined in Ref. 11. This agrees identically with the result obtained by Waugh[17] using an alternative approach due to Hurrell. Oscillations of the mass flow rate for small-amplitude disturbances are easily calculated with this formula.

Oscillations of mass flow rate in diffuser A have also been computed, giving the results shown in Fig. 8. A pressure disturbance with frequency 300 Hz and amplitude 10% of the average pressure causes the airflow rate to fluctuate with an amplitude of nearly 3%. If the fuel flow rate remains constant, this implies that the equivalence ratio will fluctuate with the same amplitude. This will obviously affect the downstream combustion processes. Unlike the predictions of linear theory, the amplitude of mass flow oscillation is smaller for disturbances with higher amplitude. This is due to the fact that nonlinear effects tend to displace the shock toward the throat and reduce its strength.

Upstream Disturbances

Pressure oscillation originating upstream of the shock due to unsteady boundary layers or changes in flight conditions may be important. Their influences on shock motion and the downstream flowfield are discussed in this section. A linear analysis is first carried out, followed by a numerical nonlinear analysis.

In contrast to the problem dealt with in the earlier work,[11] the shock motion studied here is due to upstream disturbances. Thus, the fluctuations of velocity in a frame moving with the shock and pressure just upstream of the shock are

$$u_1' = u_e' - v_s' + \frac{d\bar{u}_1}{dx}x_s' \tag{12}$$

$$p_1' = p_e' + \frac{d\bar{p}_1}{dx}x_s' \tag{13}$$

respectively, where the last terms on the right-hand sides are due to shock motion in a nonuniform flowfield, and the subscript e denotes the incident disturbance. Similarly, the fluctuating velocity and pressure immediately downstream of the shock are

$$u_2' = u_1' - v_s' + \frac{d\bar{u}_2}{dx}x_s' \tag{14}$$

$$p_2' = p_1' + \frac{d\bar{p}_2}{dx}x_s' \tag{15}$$

Substituting the above expressions [Eqs. (12-15)] into the normal shock relations and assuming quasisteady behavior for the shock, the following formula is obtained for the transmission coefficient of a shock, T_r:

$$T_r \equiv \frac{p_1'}{p_e'} = \left[\frac{\sigma_1 + i\Omega\sigma_2}{\sigma_3 + i\Omega\sigma_4}\right]\frac{\bar{M}_1}{\bar{M}_2} \tag{16}$$

where

$$\sigma_1 = \frac{2+(1-\gamma)\bar{M}_1^2}{(\gamma+1)\bar{M}_1^2}P_s + \gamma\bar{M}_2\left(\frac{\bar{a}_2}{\bar{a}_1}\right)\left[1+\frac{4\bar{M}_1}{\gamma+1}\left(\frac{\bar{p}_1}{\bar{p}_2}\right)\right]U_s \tag{17}$$

$$\sigma_2 = -\frac{2\gamma}{\gamma+1}\left(\frac{\bar{a}_2}{\bar{a}_1}\right)\left[2\bar{M}_1\left(\frac{\bar{p}_1}{\bar{p}_2}\right)+\frac{\bar{M}_1^2+1}{\bar{M}_1^2}\right] \tag{18}$$

$$\sigma_3 = \gamma\bar{M}_2U_s - P_s \tag{19}$$

$$\sigma_4 = \frac{-2\gamma}{\gamma+1}\left[1+\frac{1}{\bar{M}_1^2}+2\bar{M}_2\right] \tag{20}$$

Figures 9 and 10 show the magnitude and phase of the transmission coefficient T_r. The result is well known: the shock amplifies all the disturbances from upstream. The magnitude of T_r is always greater than unity, and increases with the shock strength.

Numerical calculations for finite disturbances have shown that the dependence of the shock motion on amplitude and frequency are similar to those for downstream disturbances.

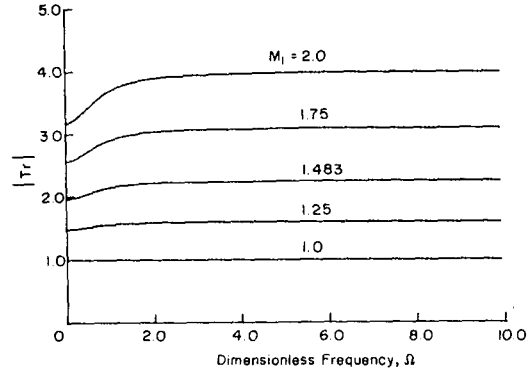

Fig. 9 Magnitude of transmission coefficient, T_r.

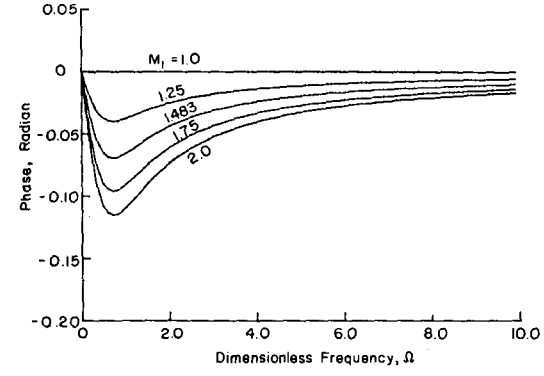

Fig. 10 Phase of transmission coefficient, T_r.

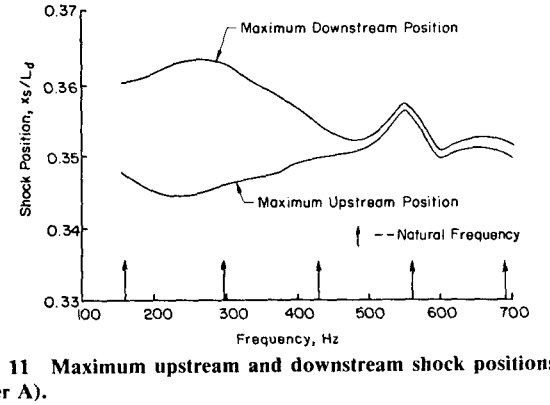

Fig. 11 Maximum upstream and downstream shock positions (diffuser A).

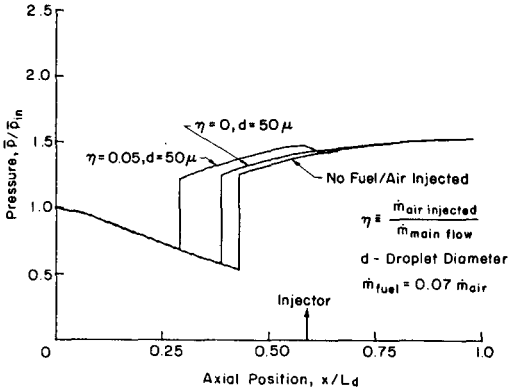

Fig. 12 Mean pressure distributions under various injection conditions (diffuser B).

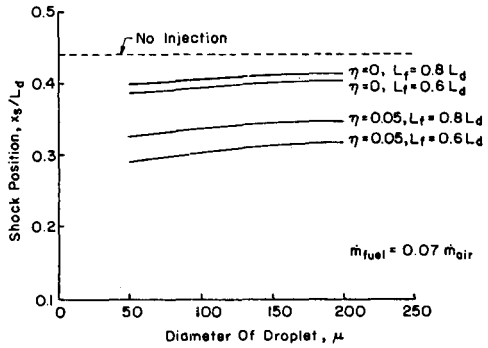

Fig. 13 Dependence of shock position on droplet size and injector position (diffuser B).

The average position of shock wave is always shifted upstream.

Resonance

One of the important issues regarding the oscillatory pressure field in an acoustic cavity is resonance. With supersonic flow upstream of the shock in an inlet diffuser, the cavity is defined as the region from the shock to the exit, where the counter-running wave system exists. Calculation of the natural frequencies is straightforward using a linear one-dimensional acoustic model. If we assume that the cross-sectional area of the diffuser varies slowly, then the appropriate equation describing the acoustic pressure field is

$$P=\frac{p'}{\gamma\bar{p}}=\sqrt{\frac{\bar{a}^2-\bar{u}^2}{\bar{a}}}\left\{P_+\exp\left[-i\omega t+i\omega\int_{L_f}^{x}\frac{dx'}{\bar{a}+\bar{u}}\right]\right.$$
$$\left.+P_-\exp\left[-i\omega t-i\omega\int_{L_f}^{x}\frac{dx'}{\bar{a}-\bar{u}}\right]\right\} \qquad (21)$$

where P_+ and P_- are complex amplitudes of the right- and left-running waves. By applying the condition for reflection at the shock and treating the exit as an acoustic node, the following transcendental equation for the natural frequencies is obtained:

$$\beta\exp\left[i\omega\int_{L_f}^{L_d}\frac{dx'}{\bar{a}+\bar{u}}\right]+\exp\left[-i\omega\int_{L_f}^{L_d}\frac{dx'}{\bar{a}-\bar{u}}\right]=0 \qquad (22)$$

where β is the acoustic reflection coefficient at the shock given in Ref. 11.

To check if resonances exist, numerical calculations have been carried out for periodic pressure oscillations with a wide range of frequencies imposed at the entrance. Figure 11 shows the spectra of the extreme excursions of the shock in diffuser A with $\delta p=0.1\bar{p}_{in}$, where the vertical arrows indicate natural frequencies determined from Eq. (22). Only near the fourth harmonic (560 Hz) does the shock response (weakly) resemble that for resonance. The shock is an overdamped system. A similar conclusion has been reached by Sajben and Bogar[3] in their experimental investigation of forced oscillation in supercritical diffuser flows.

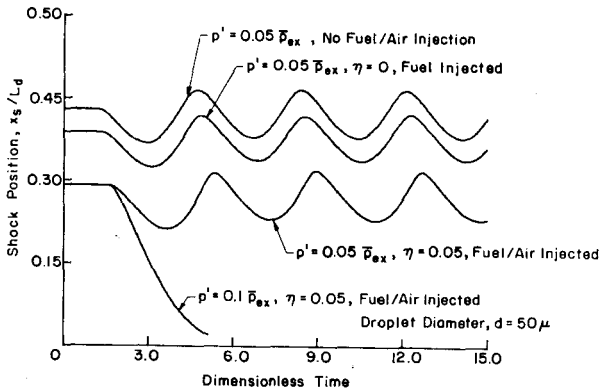

Fig. 14 Instantaneous shock position due to downstream disturbance with $f=300$ Hz (diffuser B).

Influence of Fuel and Air Injections

Thus far only the behavior of a single-phase flow has been examined. For many practical ramjet engines, fuel is injected and atomized in the inlet section. Thus, it is necessary to examine the flowfield with liquid fuel droplets accounted for. Calculations have been done for various drop sizes, injector locations, and airflow rates through the injector, while keeping the boundary conditions and fuel-to-air ratio fixed. Figure 12 shows the mean pressure distributions in diffuser B with stoichiometric RJ-4 fuel droplets ($\dot{m}_{fuel}=0.07\dot{m}_{air}$) and wall air jet introduced. The injected fuel/airflow modifies the main flowfield noticeably, moving the shock upstream and reducing the shock strength. The mean shock positions for various injection conditions are shown in Fig. 13. The effects of fuel droplets are measured best by their momentum and heat transfer to the gas flow. Since smaller droplets mean a greater specific surface area for a mixture with fixed fuel-to-air ratio, the effects increase with decreasing droplet size. Evidently the dependence of shock position on the rate of mass injection is the dominant effect.

Figure 14 shows the instantaneous shock positions subject to downstream disturbances. A comparison between Figs. 6 and 14 clearly indicates that the stability margin of a shock is reduced by injecting fuel and air into the main flow. A pressure disturbance with $\delta p=0.1\bar{p}_{ex}$ forces the shock to pass through the throat in a flow with a small amount of air added ($\eta=0.05$), while the stability is ensured even for $\delta p=0.15\bar{p}_{ex}$ in a flow without injection.

Concluding Remarks

The numerical analysis described here serves as a convenient and inexpensive means of assessing the influence of large-amplitude disturbances on the unsteady behavior of an inlet diffuser. It is not the intention of this work to provide a theory of the diffuser, but rather to construct an approximate representation which may later be used in analysis of the nonlinear behavior of an entire engine. Because viscous effects have been ignored, any results obtained with the formulation used here are restricted to relatively weak shocks so that flow separation does not occur.

Acknowledgments

The authors are indebted to J. N. Levine for providing the updated numerical code for the self-adjusting hybrid scheme. This work represents a part of the results obtained from the research program supported partly by the California Institute of Technology and partly by the Air Force Office of Scientific Research, Grant AFOSR-80-0265.

References

[1]Culick, F. E. C., "Report of the JANNAF Workshop on Pressure Oscillations in Ramjets," 17th JANNAF Combustion Meeting, CPIA Publication No. 329, Vol. III, Nov. 1980.

[2]Chen, C. P., Sajben, M., and Kroutil, J. C., "Shock-Wave Oscillations in a Transonic Diffuser Flow," *AIAA Journal*, Vol. 17, Oct. 1979, pp. 1076-1083.

[3]Sajben, M. and Bogar, T. J., "Unsteady Transonic Flow in a Two-Dimensional Diffuser: Interpretation of Experimental Results," McDonnell Douglas, St. Louis, Mo., Final Report, MDC-Q-0799, March 1982.

[4]Bogar, T. J., Sajben, M., and Kroutil, J. C., "Characteristic Frequencies of Transonic Diffuser Flow Oscillations," *AIAA Journal*, Vol. 21, Sept. 1983, pp. 1232-1240.

[5]Schadow, K. C., Crump, J. E., and Blomshield, F., "Combustion Instability in a Research Dump Combustor: Inlet Shock Oscillations," 18th JANNAF Combustion Meeting, CPIA Publication No. 343, Vol. III, Oct. 1981.

[6]Adamson, T. C. Jr., Messiter, A. F., and Liou, M-S., "Large Amplitude Shock-Wave Motion in Two-Dimensional Transonic Channel Flow," *AIAA Journal*, Vol. 16, Dec. 1978, pp. 1240-1247.

[7]Liou, M-S. and Sajben, M., "Analysis of Unsteady Viscous Transonic Flow with a Shock Wave in a Two-Dimensional Channel," AIAA Paper 80-0195, 1980.

[8]Liou, M-S., "Analysis of Viscous-Inviscid Interaction in Transonic Internal Flows," *AIAA Journal*, Vol. 21, July 1983, pp. 962-969.

[9]Liu, N-S., Shamroth, S. J., and McDonald, H., "Numerical Solutions of Navier-Stokes Equations for Compressible Turbulent Two/Three Dimensional Flows in the Terminal Shock Region of an Inlet/Diffuser," NASA-CR-3723, 1983.

[10]Liou, M-S. and Coakley, T. J., "Numerical Simulations of Unsteady Transonic Flows in Diffusers," AIAA Paper 82-1000, 1982.

[11]Culick, F. E. C. and Rogers, T., "The Response of Normal Shocks in Diffusers," *AIAA Journal*, Vol. 21, Oct. 1983, pp. 1382-1390.

[12]Levine, J. N. and Culick, F. E. C., "Nonlinear Analysis of Solid Rocket Combustion Instability," AFRPL TR-74-45, 1974.

[13]Chen, D. Y., Yang, V., and Kuo, K. K., "Boundary Condition Specification for Mobile Granular Propellant Bed Combustion Processes," *AIAA Journal*, Vol. 19, Nov. 1981, pp. 1429-1437.

[14]Baum, J. D. and Levine, J. N., "Evaluation of Finite Difference Schemes for Solving Nonlinear Wave Propagation Problems in Rocket Combustion Chambers," AIAA Paper 81-0420, 1981.

[15]Harten, A., "The Artificial Compression Method for Computation of Shocks and Contact Discontinuities: III, Self Adjusting Hybrid Schemes," AFOSR TR-77-0659, 1977.

[16]Richtmyer, R. D. and Morton, K. W., *Difference Methods for Initial-Value Problems,* 2nd ed., Interscience Publishers, New York, 1969.

[17]Waugh, R. C., "Inlet Response to Acoustic Oscillations," Appendix C, Ramjet Combustor Instability Investigation: Literature Survey and Preliminary Design Study, prepared by R. C. Waugh et al., United Technologies, Sunnyvale, Calif., Rept. CSD-2770-IR-1, Jan. 1982.